

Astronomical Diffuse Interstellar Bands Analyzed by Hydrocarbon Pentagon-Hexagon Combined PAH Molecules

Norio Ota

Graduate school of Pure and Applied Sciences, University of Tsukuba, 1-1-1 Tennodai, Tsukuba-City Ibaraki 305-8571, Japan

Web: <https://www.researchgate.net/profile/Norio-Ota-Or-Ohta>

This study theoretically predicted the specific Polycyclic Aromatic Hydrocarbon (PAH) molecules to satisfy both astronomically observed Diffuse Interstellar Bands (DIB) and Infrared Bands (IR). Under astronomical top-down material creation scheme, we have previously found the hydrocarbon pentagon-hexagon combined PAH molecules by comparing observed IR with Density Functional Theory (DFT) calculated molecular vibrational spectrum. Molecules were ($C_{53}H_{18}$), ($C_{23}H_{12}$) and ($C_{12}H_8$). Origin of DIB may come from the photoexcitation between molecular orbitals. For those molecules, we calculated excitation energy by the time dependent DFT. In case of ($C_{53}H_{18}$), mono cation shows calculated 722nm excitation band coincide well with observed DIB at 722.31nm, also calculated 693nm coincide with observed 693.90nm. Di-cation one also shows good coincidence by calculated 864nm with 864.82nm DIB. For middle sized molecule ($C_{23}H_{12}$), mono cation shows calculated 617nm coincidence with observed 617.73nm, also calculated 645nm with observed 645.16nm. Smaller sized di-cation molecule of ($C_{12}H_8$) show calculated band of 440nm roughly related to observed 442.89nm DIB. By this study, we could indicate the pentagon hexagon combined PAH would be promising candidate floating in interstellar space.

Key words: DIB, IR, PAH, TD-DFT,

1. Introduction

This paper firstly reports to indicate background molecules to coincide with both astronomically observed infrared emission bands (IR) and visible to near-infrared absorption band. Such absorption band were called Diffuse Interstellar Bands (DIB) as reviewed by T. R. Geballe¹⁾. In our recent paper²⁾, specific PAHs coincide with observed IR were selected under the astronomical top-down material creation model³⁾ by comparing with the density functional theory (DFT) based calculation on polycyclic aromatic hydrocarbon (PAH) molecules. Obtained PAHs were ($C_{53}H_{18}$), ($C_{23}H_{12}$) and ($C_{12}H_8$), which has one or two pentagon hydrocarbon units among hexagon networks. In this study, we expected that those molecules may contribute again on DIB. It was assumed that DIB may come from the photoexcitation (absorption) between molecular orbitals, which may show specific bands for individual molecule. We tried the time dependent density functional theory (TD-DFT) analysis.

To identify specified PAH, we did paradigm shift from the bottom-up astronomical dust creation scheme to the top-down one. Those were reviewed by A. Tielens³⁾ in 2013. Conventional bottom-up process was that few atoms create larger molecule one by one as like laboratory chemical reaction. For example, C_2 chemically reacts with C_4 to result C_6 . On the other

hand, the top-down creation was physical transformation of larger molecule to smaller one as like laboratory physical sputtering, for example from C_{10} to C_9 by high-speed proton attack. We already applied this top-down scheme to molecular vibrational IR and show successful coincidence²⁾ with well-known astronomical PAH bands in a wide wavelength from 3.2, 6.3, 7.7, 8.6, 11.2, to 12.7 micrometer⁴⁾⁻¹¹⁾. Recent review was opened by A. Li¹²⁾ in 2020.

The Diffuse Interstellar Bands (DIB) are a large set of absorption features at optical and near infrared wavelengths to be supposed associated with carbon-based molecules. The discovery of the first diffuse interstellar bands was made by Mary Lea Heger¹³⁾, almost a century ago. Until now, there observed over 500 DIBs¹⁴⁾⁻¹⁹⁾. However, any specified molecule had not been identified. In 2015, four near-infrared DIBs were matched to the laboratory spectrum of singly cationic fullerene C_{60}^{+} ²⁰⁾⁻²³⁾. However, others were not identified yet. This is the great mystery for the astrochemistry and molecular science.

Purpose of this study is to indicate the candidate molecule to satisfy both astronomically observed IR and DIB.

2. Top-Down Scheme

We followed astrophysical dust creation model. The first supposition is the creation of super giant molecule after death of large star. Just after star

explosion, high temperature carbon plasma was released to circumstellar space as imaged in Fig. 1. There causes cooling of plasma and collision with previously emitted dust cloud, resulting the creation of super giant carbon molecule. Nozawa et al.⁽²⁴⁾⁽²⁵⁾ calculated the chemical composition, size distribution, and amount of dust grains formed in the ejecta of population III super novae. After 10^5 years, there remain carbon dust with size from 1 to 10 nm, which suggests 100 to 10000 carbons super giant molecule. At a high temperature plasma condition, large carbon molecules would be created as studied in laboratory⁽²⁶⁾⁽²⁷⁾ and by simulation⁽²⁸⁾. After such events, those giant carbon molecule, sometimes may be reacted with hydrogen cloud, and transformed to large size PAHs.

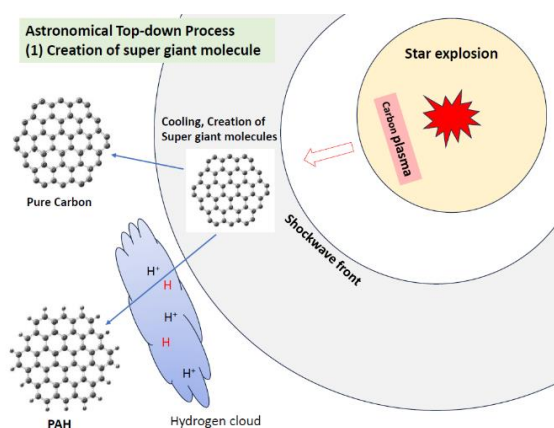


Fig. 1 Image of creating super giant carbon and/or PAH molecules after the star explosion.

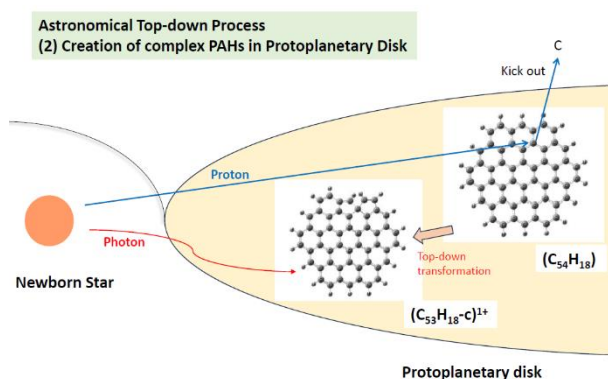


Fig. 2 Image of creation of pentagon hexagon combined large PAH by high-speed proton attack, and high energy photon radiation from newborn central star.

A capable second step would be realized at the star born age, as like inside of protoplanetary disk⁽²⁹⁾⁽³⁰⁾ as shown in Fig. 2. Floating PAH would be attacked by high-speed particles as like proton and/or electrons emitted from newborn central star. Carbon atom in a molecule will be kicked out to result new deformed

molecule, complex PAHs. Typical example was shown in Fig. 2 that full hexagon hydrocarbon ($C_{54}H_{18}$) will be transformed to ($C_{53}H_{18}$) having two pentagons among many hexagons. Also, central star illuminates high energy photon on those transformed PAH, which extract electron to result cationic PAH, as like mono-cation, di-cation and so on⁽³⁰⁾. Complex PAH and its family would be easily created by such simple physical top-down processes.

3. Molecular Vibrational Infrared Bands

In our previous papers⁽²⁾⁽³⁰⁾ under the top-down scheme, we successfully indicated specific molecule group. Fig. 3 is typical comparison of observed astronomical spectra and DFT calculated bands. Left upper panel show typical spectrum of four objects, so called PAH type bands of 3.2, 6.3, 7.7, 8.6, 11.2, and 12.7 micrometer. We can see good coincidence with calculated bands of ($C_{53}H_{18-c}$)¹⁺ as noted in Ref. 2. Suffix -c was substituted carbon position on original molecule of ($C_{54}H_{18}$), in this paper suffix is abbreviated for simplicity. Also, middle sized molecule of ($C_{23}H_{12}$)²⁺ show fair agreement in wide wavelength range from 3.3 to 12.7 micrometer. Observed spectrum would be sum of those top-down scheme molecular group, which may depend on environmental situation of central star size, temperature, distance etc. Right hand top panel show very young star's observed spectrum. Against such complex spectrum⁽²⁾⁽³⁰⁾, we could find suitable molecule to be di-cation ($C_{12}H_8$)²⁺. It was amazing to predict specified background molecules under such top-down scheme.

4. Calculation Methods

In calculation, we used DFT^(31,32) and TD-DFT with the unrestricted PBEPBE functional^(33), 34). We utilized the Gaussian09 software package⁽³⁵⁾ employing an atomic orbital 6-31G basis set⁽³⁶⁾. Unrestricted DFT calculation was done to have the spin dependent atomic structure. The required convergence of the root-mean-square density matrix was 10^{-8} . Based on such optimized molecular configuration, fundamental vibrational modes were calculated. This calculation also gives harmonic vibrational frequency and intensity in infrared region. The standard scaling is applied to the frequencies by employing a scale factor of 0.975. Correction due to anharmonicity was not applied to avoid uncertain fitting parameters. To each spectral line, we assigned a Gaussian profile with a full width at half maximum (FWHM) of 4cm^{-1} . For obtaining the molecular orbital excitation energy and strength, we tried up-to 14th excitation on TD-DFT calculation of Gaussian09.

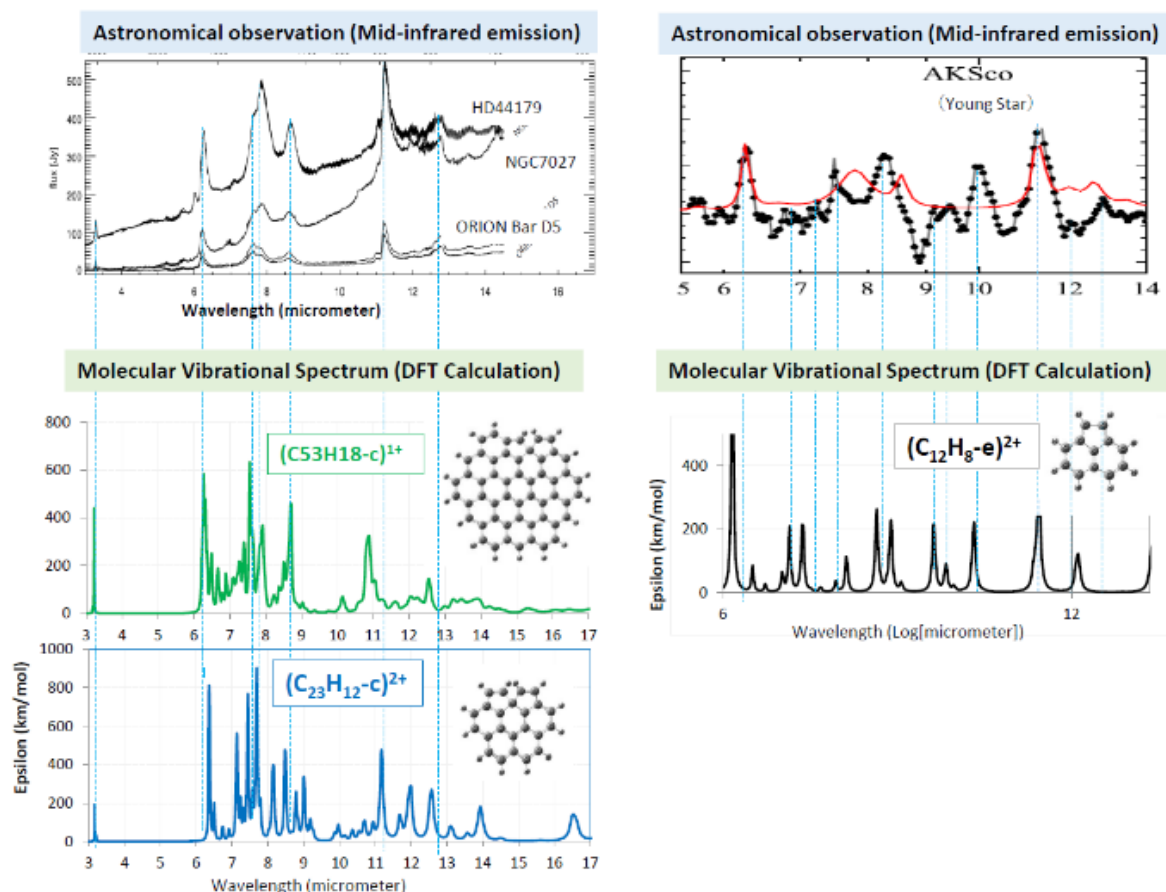


Fig. 3 Observed infrared spectrum compared with DFT calculated spectrum of the hydrocarbon pentagon-hexagon combined PAHs.

5. Molecular Orbitals and Excitation Energy

Typical example of molecular orbital calculation was illustrated in Fig. 4 for a case of $(C_{53}H_{18})^{1+}$. Optimization of molecular configuration and mapping of spin density was done by DFT. In panel (a), we can see configuration with two hydrocarbon pentagons among hexagon networks. In panel (b), up-spin cloud (by red) and down-spin one (blue) was mapped. Up-spin rich arrangement was appeared around pentagon sites. By TD-DFT calculation, molecular orbital energy diagram was obtained as shown in (c). HOMO orbit was number-167 (#167) for up-spin alpha bands (marked by red arrow) and down-spin beta band (blue arrow). LUMO was #168 for both bands. Also, we obtained photoexcitation energy among those molecular orbits. Lowest one was absorption named N1 from Beta #167 (HOMO) to #168 (LUMO), which photon energy is $N1=2659\text{nm}$ in wavelength. Second one was $N2=1591\text{nm}$ from Beta#166 to #168. Third one was $N3=1083\text{nm}$. Other higher excitation energy was calculated until 14th as N14.

It is important supposition in this study that photon excitation energy (in wavelength) would be related to astronomically observed DIB bands. Molecular orbits were illustrated in (d) for Beta HOMO and LUMO, where orange cloud show plus-sign orbit and green cloud for anti-sign one.

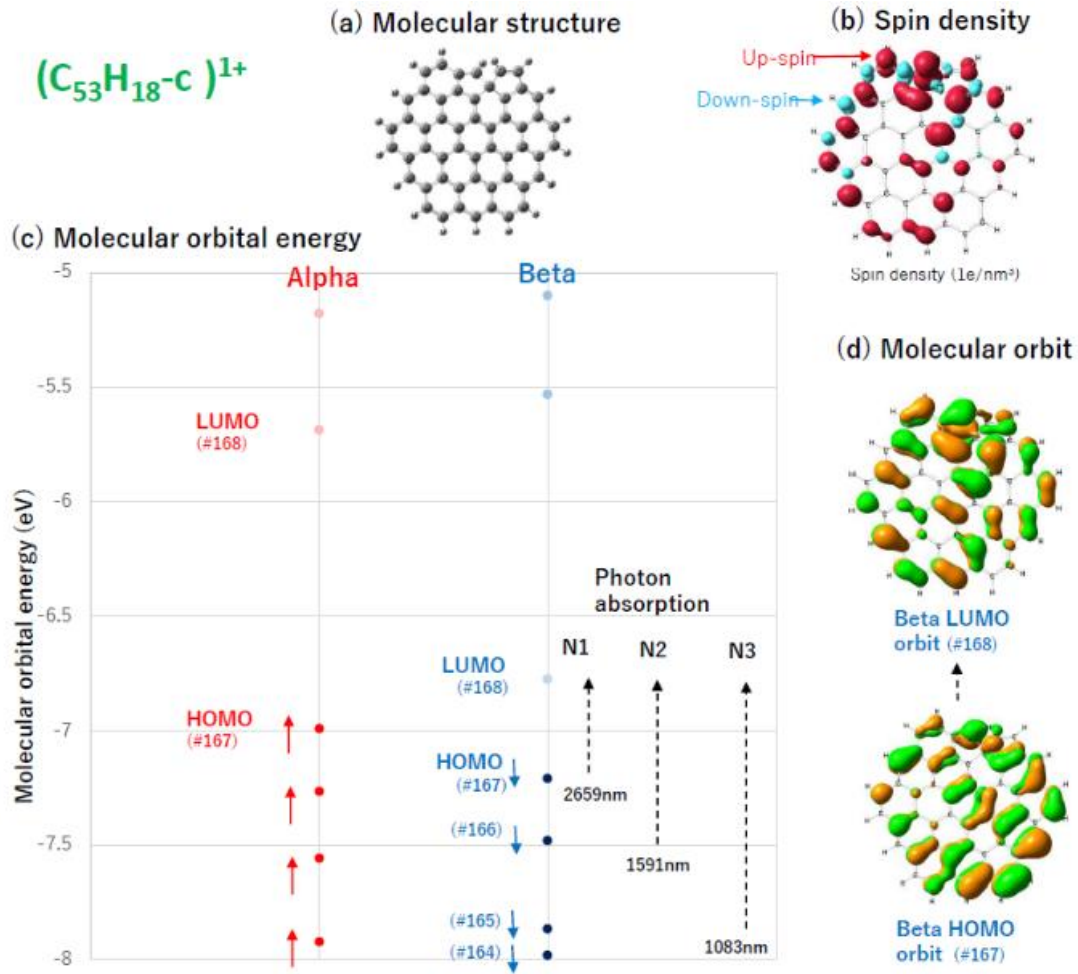


Fig. 4 DFT calculated molecular configuration of $(C_{53}H_{18})^{1+}$ was illustrated in (a), and spin density in (b). TD-DFT calculated molecular orbital energy diagram was shown in (c) for up-spin Alpha bands by red arrows and down spin Beta one by blue. Photon excitation energy in wavelength were calculated as N1, N2, N3 up to N14, which would be related to astronomically observed DIB bands. Molecular orbitals were mapped in (d), where orange cloud shows plus-sign orbit and green cloud for anti-sign one. LUMO orbit became complex structure than HOMO.

6. Molecular Orbital Excitation Energy Compared with Observed DIB

6.1 Mono-cation $(C_{53}H_{18})^{1+}$

Typical TD-DFT calculated molecular orbital photoexcitation energy was shown in Fig. 5 by wavelength in nanometer for mono-cation $(C_{53}H_{18})^{1+}$. In the lower panel, photoexcitation from number N2 to N14 were illustrated by green lines. Vertical axis is

normalized absorbed oscillating strength ($\times 10^{-4}$), which may be related with observed DIB absorption depth. Observed DIB band was shown on top left column which is synthetic DIB spectrum edited by Lan et al. in 2015³⁷⁾ based on work by Jenniskens et al. in 1994³⁸⁾ from wavelength range from 400 to 900nm. We marked deeper DIB bands from “a” to “i” in red character. Also, we listed those major observed band and calculated excitation wavelength in Table 1, where FWHM is full observed width at a half maximum, W is equivalent width related to column density of DIB carriers, $E(B=V)$ is reddening of the astronomical object. We can find fair agreement with deeper observed band-b (722-727nm) by calculated band N7 (722nm), also band-c (623nm) with N8 (623nm). In a range of 900-1000nm we had calculated N4 and N5, where is famous range for exceptionally identified specific molecule of C_{60}^{+} ^{22),23)}. Recently, DIB bands were observed in near-infrared and infrared region (1100 to 1800nm) by many observers as like Rawlings et al.³⁹⁾, Geball et al.⁴⁰⁾ and Sarre et al.⁴¹⁾.

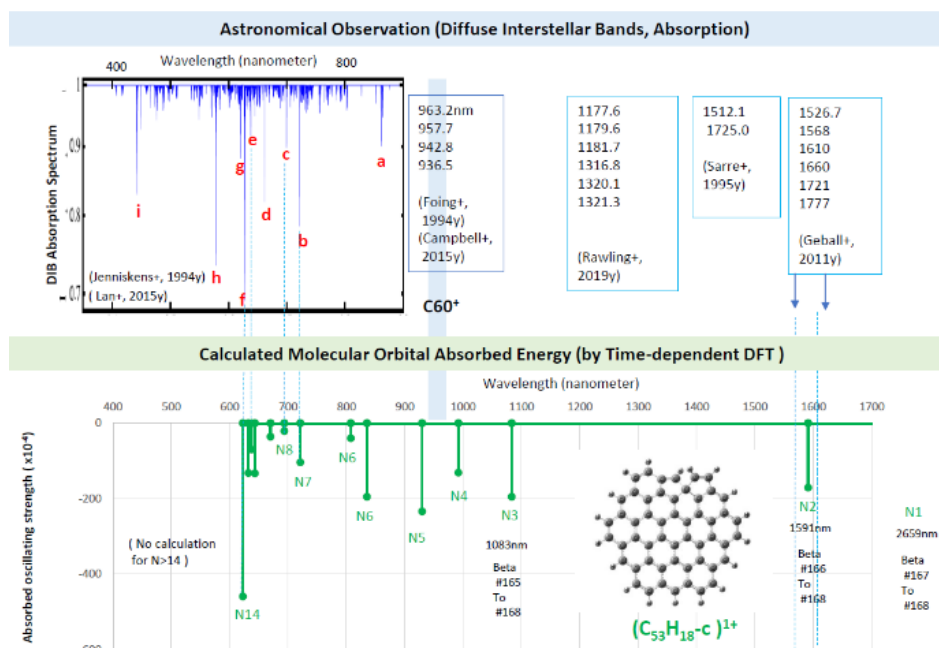


Fig. 5 TD-DFT calculated molecular photoexcitation bands for (C₅₃H₁₈)¹⁺ on lower panel, compared with observed DIB bands on upper panel.

Table 1, Comparison of observed major DIB bands (in left, blue panel) with TD-DFT calculated molecular photoexcitation absorbed bands (in right, green panel).

DIB band	Observation (by Jenniskens et al.)			Calculation (This work)				
	Wavelength (nm)	FWHM (nm)	W/E(B-V)	Wavelength (nm)	Polarized strength (10E-4)	Molecule A, Charge	Molecule B, Charge	Molecule C, Charge
						(C53H18-c)	(C23H12-c)	(C12H8)
a	864.82	0.42	0.24	864	-218	A, 2+		
	862.12	0.56	0.27					
b	727.45	0.51	0.06	724	-274		B, 1+	
	722.42	0.11	0.26	722	-104	A, 1+		
	722.31	0.54	0.08					
c	693.90	2.13	0.39	695	-481	A, 2+		
				693	-21	A, 1+		
				690	-107	A, 0+		
d	653.21	1.72	0.66					
	649.42	1.12	0.2					
	645.16	2.54	0.4	645	-631	A, 2+		
e	635.95	3.73	0.53	643	-133	A, 1+		
f	628.43	0.26	0.62	624	-379	A, 2+		
	628.11	0.84	1.23	622	-459	A, 1+		
g	617.73	2.3	0.77	617	-43		B, 1+	
h	578.06	0.2	0.58	586	-756	A, 0+		
	577.95	1.55	0.65	580	-464	A, 2+		
i	442.89	1.23	2.23	442	-549		B, 2+	
				440	-42			C, 2+

6.2 Large size molecule ($C_{53}H_{18}$)ⁿ⁺

Our previous paper²⁾ suggested that neutral and cationic state of ($C_{53}H_{18}$) contribute on observed IR as illustrated on right side of Fig.6. Here, we should study charged state dependence on molecular photoexcitation bands. On left side of Fig. 6, we compared observed DIB with calculated photoexcitation of ($C_{53}H_{18}$)ⁿ⁺ (n=0, 1 and 2). Neutral molecule ($C_{53}H_{18}$)⁰⁺ show calculated band at 690nm and 586nm, which are close to observed band-c (693.90nm) and band-h (578.06nm). Concerning di-cation molecule ($C_{53}H_{18}$)²⁺, calculated band of 864nm may contribute on band-a (864.82nm), calculated 695nm on band-c (693.90nm), and calculated 580nm on band-h (578.06nm). We can see detailed comparison in Table 1.

6.3 Middle size molecule ($C_{23}H_{12}$)ⁿ⁺

Middle size molecule of ($C_{23}H_{12}$)ⁿ⁺ (n=0, 1 and 2) was studied as shown in Fig. 7. Previously studied IR spectrum²⁾ was copied on right panel. Di-cation one revealed close band structure with observed IR. Of course, neutral and mono-cation molecules would partly contribute on observed spectrum. For those candidates, we tried again TD-DFT calculation. Results were noted on left side of Fig. 7 and Table 1. Calculated band of mono-cation at 724nm may belong to observed band-b (722.31nm), also calculated band at 617nm belong to band-g (617.73nm). Calculated band of di-cation molecule at 442nm may belong to observed band-i (442.89nm).

6.4 Small size molecule ($C_{12}H_8$)ⁿ⁺

As a typical smaller size candidate, ($C_{12}H_8$)ⁿ⁺ was studied as resulted in Fig. 8 and Table 1. Such small size molecule could not become a main contributor on visible to near-infrared wavelength region. Calculated band at 440nm by mono-cation may belong to observed band-i (442.89nm). Calculation suggested that there may be extra ultraviolet DIB bands (200 to 400nm) by those smaller size PAH's.

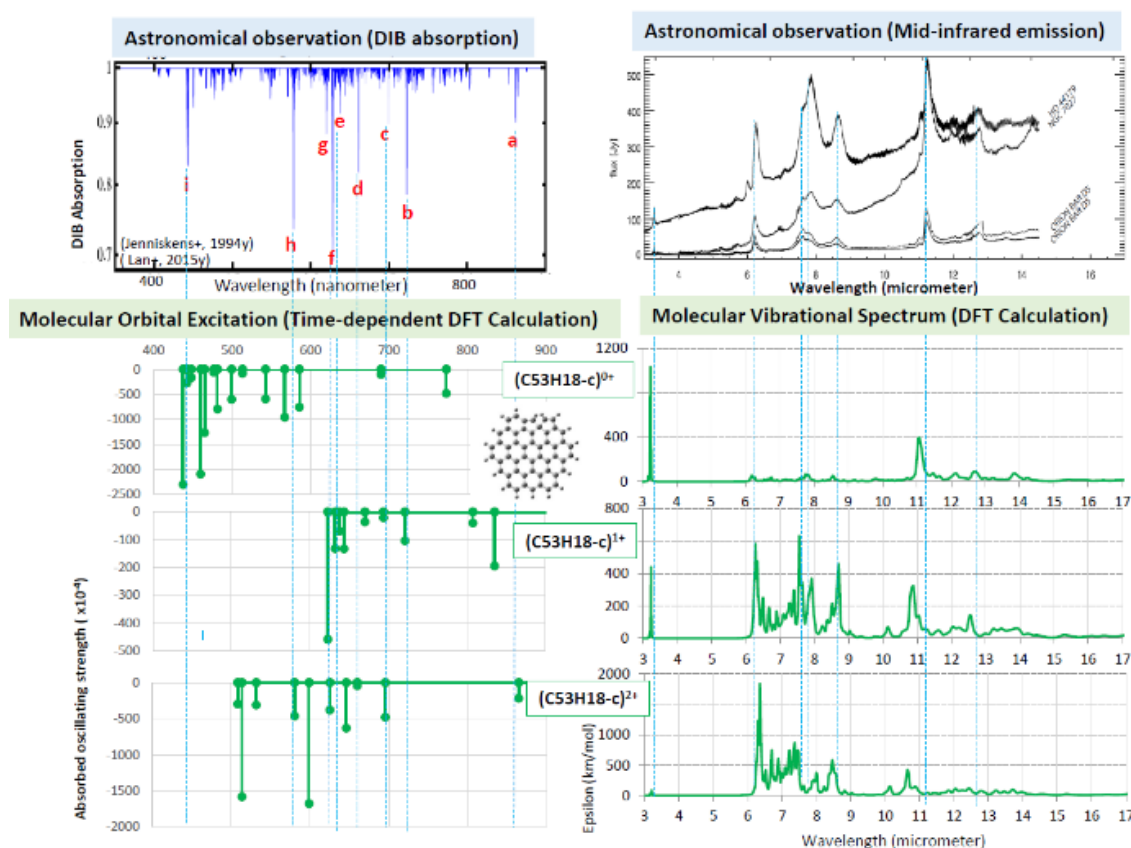


Fig. 6 Calculated infrared spectrum and molecular orbital excitation energy for ($C_{53}H_{18}$ -c)ⁿ⁺ (n=0, 1 and 2) compared with astronomical IR on right and DIB on left.

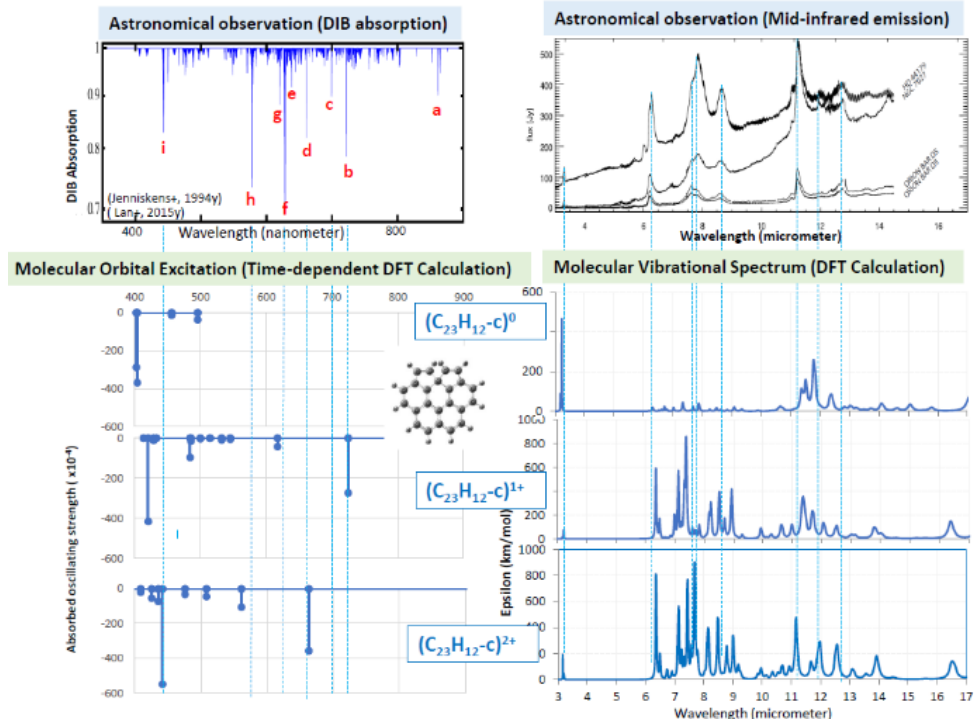


Fig. 7 Calculated infrared spectrum and molecular orbital excitation energy for $(C_{23}H_{12})^{n+}$ ($n=0, 1$ and 2) compared with observed IR and DIB.

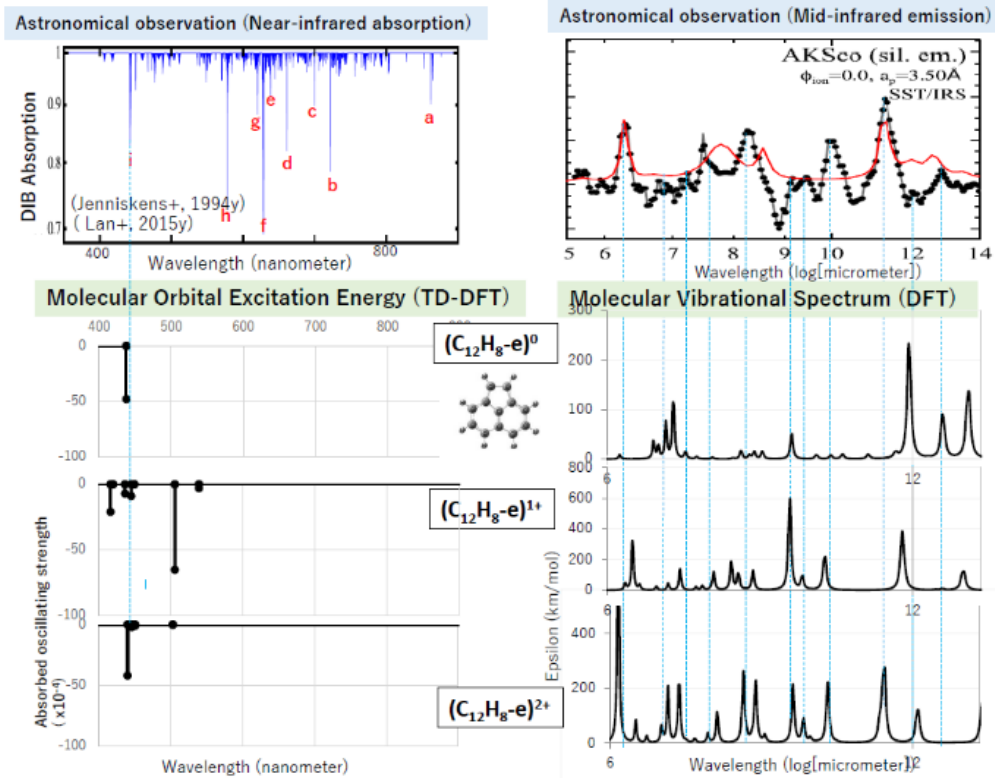


Fig. 8 Calculated IR (on right) and molecular orbital excitation energy (on left) for $(C_{12}H_8)^{n+}$ ($n=0, 1$ and 2) compared with the young star AKSco's IR and DIB bands.

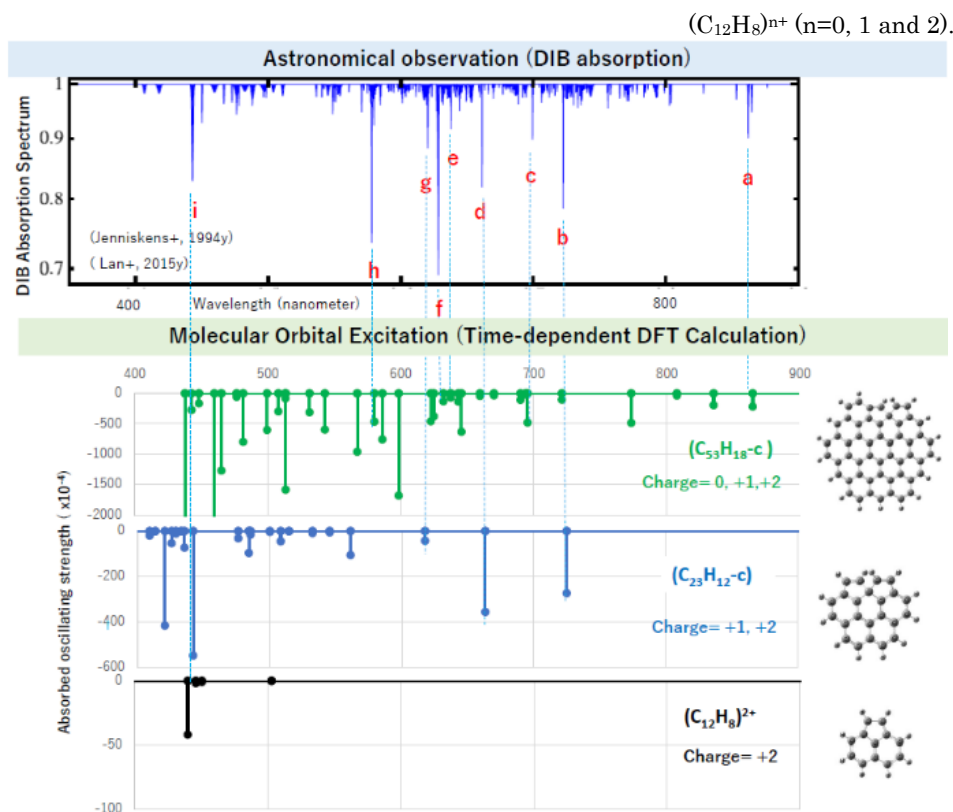


Fig. 9 Candidate molecules could reproduce observed DIB bands.

7. Reproducing DIB by Promising Molecules

We like to select specific PAH molecule to satisfy observed bands both infrared emission IR and DIB absorption spectrum. Larger molecule ($C_{53}H_{18}$) reproduces IR well by combination of neutral and mono-cation. Also, molecular orbital excitation of ($C_{53}H_{18}$) could reproduce DIB by a combination of neutral, mono, and di-cation one as listed in Table 1. Mono- and di-cation of ($C_{23}H_{12}$) could show good reproduction for both observed IR and DIB bands. Smaller molecule ($C_{12}H_8$) shows fair coincidence by only di-cation one. Under those selected species, we could compare detailed band structure as shown in Fig. 9.

8. Conclusion

Purpose of this study is to indicate specific PAH molecules to coincide both astronomically observed IR and DIB bands by DFT and TD-DFT calculation.

- (1) Under astronomical top-down material creation scheme, we have previously found the hydrocarbon pentagon-hexagon combined PAH molecules by comparing featured IR and DFT obtained molecular vibrational spectrum. Molecules were $(C_{53}H_{18})^{n+}$, $(C_{23}H_{12})^{n+}$ and

- (2) For above molecules, we obtained the molecular orbitals and photo-excitation energy, from HOMO to LUMO absorption energy and other higher absorption modes.
- (3) In case of large size molecule $(C_{53}H_{18})^{n+}$, mono-cation show calculated 722nm band coincide well with observed DIB at 722.31nm, also calculated 693nm with observed 693.90nm. Di-cation one show good coincidence by calculated 864nm with observed 864.82nm DIB, also calculated 645nm with observed 645.16nm.
- (4) For middle size $(C_{23}H_{12})^{n+}$, mono-cation calculated band at 617nm coincide well with observed 617.73nm DIB, also calculated 645nm with observed 645.16nm.
- (5) Smaller size $(C_{12}H_8)^{n+}$, calculated excitation bands were obtained in shorter wavelength region than 500nm. Only calculated band of 440nm by di-cation roughly coincide with observed 442.89nm DIB. Such smaller molecule was expected to reproduce violet DIB bands.

By this study, we could predict specified PAHs to satisfy both observed IR and DIB spectrum.

Acknowledgement

We would like to say great thanks to DR. Christiaan Boersma of NASA Ames Research and Prof. Aigen Li for best advices on astronomical

observed data, also great thanks to Dr. T.R. Geballe for his excellent review paper on opensource web site.

References

- 1) T. R. Geballe: J. of Phys.: Conference Series **728**, 062005 (2016)
- 2) N. Ota, A. Li and L. Nemes: J. Mag. Soc. Japan **45**, 86 (2021).
- 3) A. Tielens: Rev. Mod. Phys. **85**, 1021 (2013)
- 4) J. Oomens: *In PAHs and the Universe: A Symposium to Celebrate the 25th Anniversary of the PAH Hypothesis*, EAS Publications Series (2011)
- 5) C. Boersma, J. Bregman, and L. Allamandola: *ApJ* **769**, 117 (2013).
- 6) C. Moutou, K. Sellgren, L. Verstraete, and A. L'eger: *A & A*, **347**, 949 (1999).
- 7) E. Peeters, S. Hony, C. van Kerckhoven, et al.: *A&A*, **390**, 1089 (2002).
- 8) L. Armus, V. Charmandaris, J. Bernard-Salas, *ApJ*, **656**, 148 (2007).
- 9) J. Smith, B. Draine, A. Dale, et al.: *ApJ* **656**, 770 (2007).
- 10) K. Sellgren, K. Uchida and M. Werner: *ApJ* **659**, 1338 (2007).
- 11) A. Ricca, C. W. Bauschlicher, C. Boersma, A. Tielens & L. J. Allamandola: *ApJ*, **754**, 75 (2012).
- 12) A. Li: *Nature Astronomy*, **4**, 339 (2020).
- 13) M. L. Heger: *Lick Obs. Bull.* **10** 146 (1922)
- 14) G. P. Zwet and L. J. Allamandola: *Astron. Astrophys.* **146** 76 (1985)
- 15) A. Leger and L. D'Hendecourt: *Astron. Astrophys.* **146** 81 (1985)
- 16) M. K. Crawford, A. Tielens and L. J. Allamandola: *Astrophys. J.* **293** L45 (1985)
- 17) H. W. Kroto: *Science* **242** 1139 (1988)
- 18) A. L'eger, L. D'Hendecourt, L. Verstraete L and W. Schmidt: *Astron. Astrophys.* **203** 145 (1988)
- 19) A. Webster: *Mon. Not. R. Astron. Soc.* **263** 385 (1933)
- 20) J. Fulara, M. Jakobi and J. Maier: *Chem. Phys. Lett* **211** 227 (1933)
- 21) B. H. Foing and P. Ehrenfreund: *Nature* **369** 296 (1994)
- 22) B. H. Foing and P. Ehrenfreund: *Astron. Astrophys.* **319** L59 (1977)
- 23) E. K. Campbell, M. Holz, D. Gerlich and J. P. Maier: *Nature* **523** 322 (2015)
- 24) T. Nozawa, T. Kozasa, H. Umeda, K. Maeda & K. Nomoto: *ApJ*, **598**, 785 (2003)
- 25) T. Nozawa and T. Kozasa: *The Astrophysical Journal*, **648**, 435 (2006)
- 26) L. Nemes, A. Keszler, J. Hornkohl, and C. Parigger: *Applied Optics*, **44-18**, 3661 (2005).
- 27) L. Nemes, E. Brown, S. C. Yang, U. Hommerrich: *Spectrochimica Acta Part A, Molecular and Biomolecular Spectroscopy*, **170**, 145 (2017).
- 28) N. Patra, P. Kr'all, and H. R. Sadeghpour: *The Astrophysical Journal*, **785**, 6 (2014)
- 29) J. Y. Seok and A. Li: *ApJ*, **835**, 291 (2017).
- 30) N. Ota and A. Li: *arXiv.org* 2303.05645 (2023)
- 31) P. Hohenberg and W. Kohn: *Phys. Rev.*, **136**, B864 (1964).
- 32) W. Kohn and L. Sham: *Phys. Rev.*, **140**, A1133 (1965).
- 33) Perdew, J. P.; Burke, K.; Ernzerhof, M. *Phys. Rev. Lett.* **1996**, **77**, 3865–3868 (1996)
- 34) Huan Wang, Youjun He, Yongfang Li and Hongmei Su: *Phys. Chem. A* **2012**, **116**, 255–262 (2012)
- 35) M. Frisch, G. Trucks, H. Schlegel et al: Gaussian 09 package software, Gaussian Inc. Wallington CT USA (2009).
- 36) R. Ditchfield, W. Hehre and J. Pople: *J. Chem. Phys.*, **54**, 724 (1971).
- 37) T. Lan, B. Menard and G. Zhu: *Mon. Not. R. Astron. Soc.* **452** 3629 (2015)
- 38) P. Jenniskens and F. Desert: *1994 Astron. Astrophys. Suppl. Series* **106** 39 (1994)
- 39) M. G. Rawlings, A. J. Adamson, C. C. M. Marshall and P. J. Sarre: *MNRAS* **485**, 3398–3401 (2019)
- 40) T. Geballe, F. Najarro, D. Figer, B. Schlegelmilch, and D. de la Fuente: *Nature* **479** 200E (2011).
- 41) P. Sarre, J. Miles, T. Kerr, R. Hibbins, S. Fossey and W. Somerville: *Mon. Not. R. Astron. Soc.* **277** L41 (1995)

Authors Profile : Norio Ota, PhD. (太田憲雄)
 Magnetic materials and physics, Astrochemistry,
 Honorary member of the Magnetism Society of Japan,
 2010-2021: Senior Professor, Univ. of Tsukuba, Japan.
 2003-2011: Exec. Chief Engineer, Hitachi Maxell Ltd.
<https://www.researchgate.net/profile/Norio-Ota-Or-Ohta>

